Supplementary material

This document describes the hardware and software setup of our system described in "Position Tracking for Virtual Reality" paper that appeared in CVPR 2017 [3]. This document, in addition, describes how the position tracking algorithm in the paper can be extended when the receiver has multiple antennas and how the system can utilize the fact that WiFi signals are transmitted at different frequencies. The pages, sections, figures and equations are numbered as though the supplementary material is a continuation to the paper.

8. Hardware setup

We implemented WiCapture using off-the-shelf Intel 5300 WiFi cards which support three antennas. The system we used for evaluation consists of four APs and a target device equipped with WiFi cards. The target/transmitter has a $3-$antenna circular array with distance between any two antennas equal to 2.6 cm. The receiver/AP (access point) has 3-antenna linear array with distance between any two adjacent antennas equal to 2.6 cm. The WiFi chips operate with 40 MHz bandwidth.

9. Channel modeling considering all the subcarriers

In WiFi communication systems, the transmitter sends sinusoidal signals of multiple frequencies; each frequency is called a subcarrier [2]. For every WiFi packet received, any commercial WiFi chip calculates Channel State Information (CSI) which is the amplitude and phase of the signal received from all the transmitter antennas at all the frequencies. WiCapture reuses this CSI to accurately track the trajectory of the transmitter. We now extend the modeling of the CSI described in the paper by considering the signal from multiple subcarriers.

9.1. CSI calculation

Consider a particular complex sinusoid signal $\mathrm{e}^{j2\pi f_n t}$ corresponding to n^{th} subcarrier of frequency f_n emitted by the q^{th} antenna on the transmitter; here j is the complex root of -1 and t is time. This signal passes through the wireless channel, $h_{q,n}$, gets demodulated (see Eq. 14) by the local sinusoid at the receiver, and result is the CSI for that particular antenna-subcarrier pair, $\hat{h}_{q,n}$. Mathematically,

$$\hat{h}_{q,n} = \frac{1}{T}\int_0^T h_{q,n}\mathrm{e}^{j2\pi f_n t}\mathrm{e}^{-j2\pi f_n t + j\nu}\,dt = h_{q,n}\mathrm{e}^{j\nu}, \tag{14}$$

where T is time for which sinusoid is transmitted and ν is the phase of the receiver's local sinusoidal signal relative to the phase of the transmitter's sinusoidal signal (see Fig. 4).

In indoor environments, transmitted signal travels along multiple paths and the signals from all the paths superpose to form the received signal. Each path is associated with an AoD (Angle of Departure) from the transmitter and attenuation of the signal along the path. We now describe the relation between the wireless channel $h_{q,n}$ and these path parameters. For this description, we consider the circular 3-antenna array used in our prototype although the model can be extended to any arbitrary antenna array geometry.

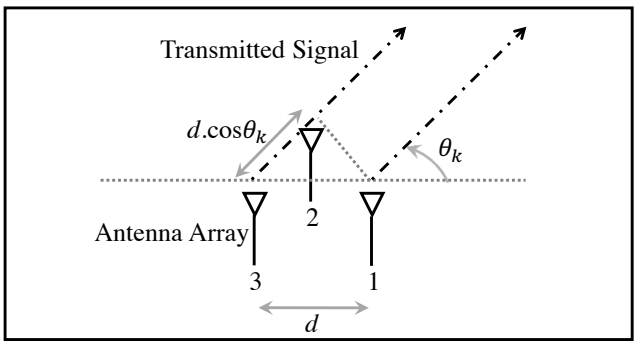

Figure 10. Uniform circular array consisting of 3 antennas: For AoD of θ_k, the target's signal travels an additional distance of $d * \cos(\theta_k)$ from the third antenna in the array compared to the signal from the first antenna. This results in an additional phase of $-2\pi * d * \cos(\theta_k)/\lambda$ for the signal received from the third antenna compared to that from the first antenna.

9.2. Wireless channel modeling for circular antenna array at the transmitter

Consider an environment with L paths; *e.g.*, setup in Fig. 5(b) has 2 paths. Let the spacing between any two antennas in the 3-antenna circular array at the transmitter be d. Let the AP/receiver be in the same plane as the transmitter antenna array. Let θ_k denote the angle of departure (AoD) from the transmitter for the k^{th} path using the convention shown in Fig. 10. Let $\gamma_{k,n}$ denote the signal received along k^{th} path from the first transmitter antenna on the n^{th} subcarrier to the receiver antenna.

The signal along k^{th} path travels different distances from different transmit antennas to the receiver and hence, the signal from different antennas accumulate different phases. So, as illustrated in Fig. 10, the vector of signals received from the transmit antennas along k^{th} path can be written as $\vec{a}(\theta_k)\gamma_{k,n}$, where

$$\vec{a}(\theta_k) = [1\ \mathrm{e}^{-j2\pi * d * \cos(\theta_k + \pi/3)/\lambda}\ \mathrm{e}^{-j2\pi * d * \cos(\theta_k)/\lambda}]^\top. \tag{15}$$

This vector $\vec{a}(\theta_k)$ is also known as the steering vector. We have as many steering vectors as the number of paths.

The overall attenuation and phase shift introduced by the environment, which is the wireless channel $h_{q,n}$, is obtained by summing the signals received from all the paths. So,

$$\mathbf{H} = [\vec{a}(\theta_1)\ \ldots\ \vec{a}(\theta_L)]\mathbf{F} = \mathbf{AF}, \tag{16}$$

where N is the number of subcarriers, $\mathbf{H} \in \mathbb{C}^{3\times N}$ is the

wireless channel matrix whose element in q^{th} row and n^{th} column is $h_{q,n}$, $\mathbf{F} \in \mathbb{C}^{L \times N}$ is the matrix of complex attenuations whose element in k^{th} row and n^{th} column is $\gamma_{k,n}$, $\mathbf{A} \in \mathbb{C}^{3 \times L}$ is the steering matrix whose k^{th} column is the steering vector for k^{th} path.

Let $\widehat{\mathbf{H}} \in \mathbb{C}^{3 \times N}$ be the observed CSI matrix whose element in q^{th} row and n^{th} column is $\hat{h}_{q,n}$. $\mathbf{H}$ would be related to the observed CSI matrix using the relation, $\widehat{\mathbf{H}} = \mathbf{H} * e^{j\nu}$ (see Eq. 14).

10. Channel modeling when APs have multiple antennas

When the access point has more than one antenna, then the signal received at multiple antennas can be used to improve the accuracy of the AoD (Angle of Departure) estimates. However, the rest of the algorithm after obtaining the AoDs of all the paths remains the same. For this description, for the receiver, we consider linear 3-antenna array that we used at the access points in our prototype although the model can be extended to any arbitrary antenna array geometry at the receiver/AP. For this description, for the transmitter, we consider uniform circular 3-antenna array that we used at the transmitter although the model can be extended to any arbitrary antenna array geometry at the transmitter. Let us consider that the signal is transmitted and received at N frequencies or subcarriers.

Consider the same L paths as discussed in the paper. Let the spacing between successive antennas in the linear array be the same d as the distance between any two antennas at the transmitter. Let ψ_k denote the angle of arrival (AoA) to the transmitter for the k^{th} path using the convention shown in Fig. 11. Let $\gamma_{k,n}$ denote the signal received along k^{th} path from the first transmitter antenna on the n^{th} subcarrier to the first antenna on the receiver.

The signal along k^{th} path travels different distances to different antennas on the receiver. So, as illustrated in Fig. 11, the vector of signals received from the first transmit antenna to all the receive antennas along k^{th} path can be written as

$$\gamma_{k,n} * [1 \; e^{-j2\pi * d * \cos(\psi_k)/\lambda} \; e^{-j2\pi * d * 2 * \cos(\psi_k)/\lambda}]^{\top}. \quad (17)$$

Extending this to the signal transmitted from all the transmitter antennas, the vector of the signals received at different receiver antennas from different transmitter antennas

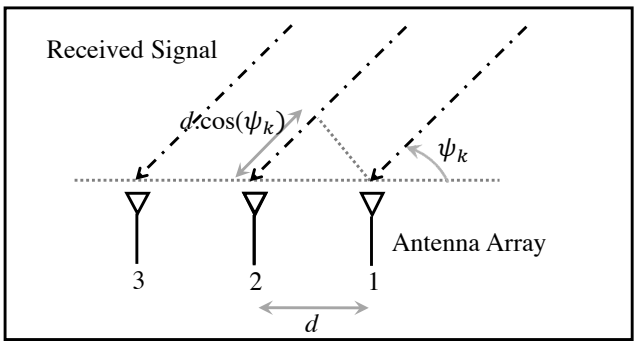

Figure 11. Uniform linear array consisting of 3 antennas: For AoA of ψ_k, the signal travels as additional distance of $d * \cos(\psi_k)$ to reach the second antenna compared to the signal received at the first antenna. This results in an additional phase of $-2\pi * d * \cos(\psi_k)/\lambda$ for the signal received from the second antenna compared to that from the first antenna.

can be written as $\vec{a}(\theta_k, \psi_k)\gamma_{k,n}$, where

$$\vec{a}(\theta_k, \psi_k) = \begin{bmatrix} 1 \\ e^{-j2\pi * d * \cos(\psi_k)/\lambda} \\ e^{-j2\pi * d * 2 * \cos(\psi_k)/\lambda} \\ e^{-j2\pi * d * \cos(\theta_k + \pi/3)/\lambda} \\ e^{-j2\pi * d * \cos(\theta_k + \pi/3)/\lambda} * e^{-j2\pi * d * \cos(\psi_k)/\lambda} \\ e^{-j2\pi * d * \cos(\theta_k + \pi/3)/\lambda} * e^{-j2\pi * d * 2 * \cos(\psi_k)/\lambda} \\ e^{-j2\pi * d * \cos(\theta_k)/\lambda} \\ e^{-j2\pi * d * \cos(\theta_k)/\lambda} * e^{-j2\pi * d * \cos(\psi_k)/\lambda} \\ e^{-j2\pi * d * \cos(\theta_k)/\lambda} * e^{-j2\pi * d * 2 * \cos(\psi_k)/\lambda} \end{bmatrix}. \quad (18)$$

In Eq. 18, the first three elements are the signals received at the receive antennas for the signal transmitted from the first antenna, the next three are the signals received for the signal from second transmit antenna and the last three elements are the signals received for the signal from third transmit antenna.

The overall attenuation and phase shift introduced by the environment, which is the wireless channel $\mathbf{H}$, is obtained by summing the signals received from all the paths. So,

$$\mathbf{H} = [\vec{a}(\theta_1, \psi_1) \; \ldots \; \vec{a}(\theta_L, \psi_L)]\mathbf{F} = \mathbf{AF}, \quad (19)$$

where N is the number of subcarriers, $\mathbf{H} \in \mathbb{C}^{9 \times N}$ is the wireless channel matrix, $\mathbf{F} \in \mathbb{C}^{L \times N}$ is the matrix of complex attenuations whose element in k^{th} row and n^{th} column is $\gamma_{k,n}$, $\mathbf{A} \in \mathbb{C}^{9 \times L}$ is the steering matrix whose k^{th} column is the steering vector for k^{th} path.

11. WiFi transceiver chain calibration

Each antenna in a WiFi chip is associated with its own transceiver chain. Channel state information is calculated by demodulating the signal that is received after passing through the transceiver chain. So, the amplitude and the phase of CSI is affected by the transceiver chain. How-

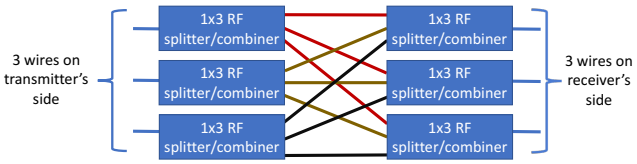

Figure 12. A wired channel that is used for calibrating transceiver responses. Each of the wires used in the circuit has a different length. The channel from each wire on the transmitter's side to each wire on the receiver's side is pre-calculated by using a Vector Network Analyzer.

ever, the effect of the transceiver chain remains the same irrespective of the environment. The transceiver chain's response manifests itself as a constant multiplicative factor in the CSI calculated by a WiFi chip. Specifically, if $\mathbf{H}$ represents the CSI obtained from the signal from different paths in the environment, then the CSI calculated by the WiFi chip can be written as

$$\mathbf{H}_{\text{wifi}} = \mathbf{H} \circ \mathbf{H}_{\text{calib}} \tag{20}$$

where $\mathbf{H}_{\text{wifi}}$ is the CSI calculated by the WiFi chip and $\mathbf{H}_{\text{calib}}$ is the multiplicative factor, which is of same dimension as $\mathbf{H}_{\text{wifi}}$, introduced by the transceiver for each of the transmit antenna - receiver antenna - subcarrier pair and $\circ$ is element-wise multiplication operation. $\mathbf{H}_{\text{calib}}$ is constant and can be calibrated out so that the system can infer the trajectory by using the signal from the environment alone without being corrupted by the transceiver chains' response.

In our prtotype, we designed the following procedure to calibrate for the transceiver chains' response. We obtain CSI calculated by the WiFi chip while the signal travels from the transmitter to the receiver along a known wired channel. We created a known wired channel by creating a circuit as shown in Fig. 12 that exposes three wires on each side; one side is called as transmitter's side and the other side is called as the receiver's side. Each of the wires used in the circuit has a different length. Using a vector network analyzer, we obtain the wired channel's response by transmitting a sinusoidal signal, with the same frequency as a subcarrier frequency and of fixed amplitude, from each of the exposed wires on the transmitter's side and measuring the amplitude and phase of the signal received at each of the exposed wires on the receiver's side. The amplitude and phase of the received signal consitute nothing but $\mathbf{H}$ corresponding to the wired channel.

Once the wired channel $\mathbf{H}$ is obtained, the wires on the transmitter's side are then connected to the WiFi chip on the transmitter and the wires on receiver's side are connected to the WiFi chip on the receiver. CSI is obtained by using the CSI tool [4] by transmitting a WiFi packet from the transmitter. This CSI $\mathbf{H}_{\text{wifi}}$ contains the effect of the wired channel and the effect of the transceiver's response according to the relation 20. By dividing each of the elements of the obtained CSI by the elements of $\mathbf{H}$ obtained from vector network analyzer, we obtain the transceiver chain's response $\mathbf{H}_{\text{calib}}$. There are multiple alternate ways to calibrate for the transceiver's response. Prior work explored developing automatic calibration procedures for calibrating the transceiver chainss response on a WiFi receiver [5]. We would like to adapt those methods to automatically calibrate the transceiver chains response on both transmitter and receiver.

12. Motion tracking algorithm when APs have multiple antennas

So, the Algorithm 1 in the main submission gets modified to Algorithm 2 to use the above model when APs have more than one antenna and use CSI on all subcarriers to improve accuracy.

Algorithm 2: WiCapture's motion tracking algorithm when there are multiple receive antennas

Data: CSI of packets from target to each of the U APs
Result: Trajectory traced by the target
Initiate the trajectory at origin ;
for *each packet p received at APs* **do**
  Consider packets received within the last V seconds. Let the number of such packets be P ;
  Form $\mathbf{X}$ from CSI of P packets using Eq. 7 in the main submission ;
  Apply MUSIC [1] on $\mathbf{X}$ to find AoD and AoA of L paths ;
  Obtain steering matrix from steering vectors formed using Eq. 18 ;
  Obtain the steering vector weights using Eq. 8 in the main submission ;
  Obtain change in complex attenuation between p^{th} and $(p+1)^{\text{th}}$ packets by solving 10 in the main submission ;
  Form $\mathbf{R}$ using Eq. 12 and $\vec{s}$ using Eq. 11 in the main submission ;
  Update the trajectory by adding displacement obtained by solving 13 in the main submission ;
end

One can observe that the algorithm remains the same except for the change in the steering vectors. Intuitively, this algorithm produces better estimates of AoD because we are constraining the CSI using both the parameters AoA and AoD instead of parameterizing it using just AoD. Further, the number of signals that can be resolved from a linear combination of steering vectors is limited by the length of each steering vector [1]. So, extending the steering vector to model the signal received at multiple receive antennas helps

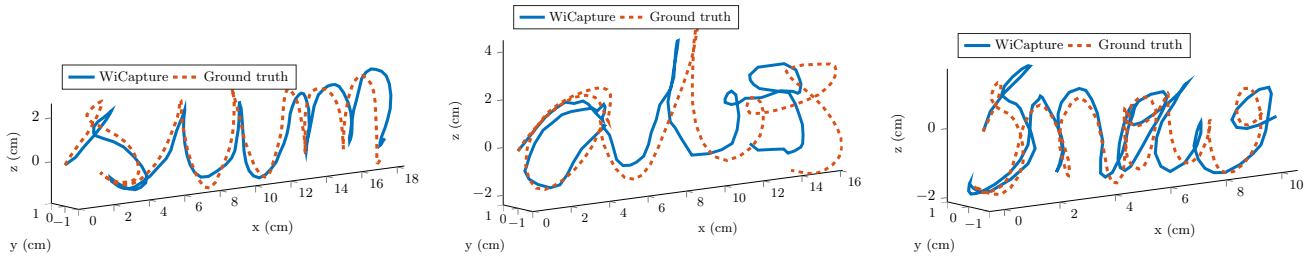

(a) Indoor office deployment (b) Occlusion deployment (c) Outdoor deployment

Figure 13. Sample traces for the three deployments

WiCapture to track the target's motion even in challenging multipath scenarios with large number of paths.

13. Sample traces

We provide a sample trace for each of the indoor office, occlusion and outdoor deployments in Fig. 13.

References

[1] R. O. Schmidt. Multiple emitter location and signal parameter estimation. *IEEE Transactions on Antennas and Propagation*, 1986.

[2] IEEE Std 802.11n-2009

[3] M. Kotaru and S. Katti. Position Tracking for Virtual Reality Using Commodity WiFi. *CVPR*, 2017.

[4] D. Halperin, W. Hu, A. Sheth, and D. Wetherall. Tool release: Gathering 802.11n traces with channel state information. *ACM SIGCOMM CCR*, 41(1):53, Jan. 2011.

[5] J. Gjengset, J. Xiong, G. McPhillips, K. Jamieson. Phaser: Enabling Phased Array Signal Processing on Commodity WiFi Access Points. *MobiCom*, 2014.